Fluorescence and NMR Studies of Human Seminal Plasma Prostatic Inhibin: Association of Lifetimes with Sterically Constrained Tryptophans

M. M. G. Krishna, Vinit K. Rastogi, N. Periasamy, and K. V. R. Chary*

Chemical Physics Group, Tata Institute of Fundamental Research, Homi Bhabha Road, Colaba, Mumbai 400 005, India

Received: October 21, 1997; In Final Form: February 10, 1998

Human seminal plasma prostatic inhibin (HSPI) is one of the first seminal plasma proteins, which has been isolated, purified, and characterized. HSPI contains two tryptophans at positions 32 and 92 along its 94 amino acid primary sequence. Among the three fluorescence quenchers acrylamide (neutral), potassium iodide (anionic), and cesium chloride (cationic), potassium iodide is found to quench the tryptophan fluorescence more compared to the other two. The fluorescence decay of HSPI is biexponential with lifetimes 5.86 and 2.44 ns. The Stern−Volmer quenching curves in the case of fluorescence intensity and average lifetime are identical, indicating that the quenching mechanism is purely dynamic. The decay associated spectra of the two lifetimes show that the two tryptophans are solvent-exposed. The fluorescence quenching data is in favor of associating the two lifetimes to separate tryptophans. The fluorescence anisotropy decay of HSPI is single exponential with a correlation time of 9.2 ns, which is due to the rotation of entire protein. Absence of any fast component in the anisotropy decay indicates that the two tryptophans are in motionally restricted, rigid environments. In NMR studies, the cross-peak patterns observed in 2D-COSY and 2D-NOESY spectra of HSPI gave unambiguous evidence that each of the two tryptophans is sterically constrained and exists in a single rotamer population.

Human seminal plasma contains a variety of proteins secreted by seminal vesicles and the prostate. Human seminal plasma prostatic inhibin (HSPI) is one of first seminal plasma proteins that has been isolated, purified, and characterized.[1] It has 94 amino acids and has a molecular weight of 10.4 kDa. HSPI has been the subject of interest for more than a decade. Its biological activity ranges from preventing pregnancy to curing prostate cancer. Inhibin prevents pregnancy in mammals by modulating the level of circulating follicle stimulating hormones (FSH).[2] It suppresses prolactin, a hormone that promotes lactation.[3] Therefore, neutralizing inhibin through active immunization leads to increase in milk production. Seidah et al. have reported the primary sequence of HSPI.[4] In the recently corrected HSPI sequence of 94 residues, all amino acid residues except alanine are present.[5] Figure 1 shows the primary structure of this protein. The number of various amino acids are as follows: Gly, 4; Val, 6; Leu, 3; Ile, 7; Asp, 7; Asn, 5; Cys, 10; Ser, 7; Thr, 8; Glu, 7; Gln, 3; Met, 1; Arg, 2; Lys, 10; Pro, 5; Phe, 2; Tyr, 4; His, 1; Trp, 2. HSPI is particularly rich in lysines and cysteines. No information is available about the three-dimensional (3D) structure of this protein. In this paper we report fluorescence and NMR studies on HSPI carried out to understand the local environment of the two tryptophans (W32 and W92) present in the protein and to obtain structural and dynamical information about the protein.

Materials and Methods

Sample Preparation. HSPI has been isolated from the semen samples of healthy men obtained at infertility clinics and purified following the well-established procedure described elsewhere.[5] The immunoactive fractions were purified by HPLC on a gel permeation preparative column (Ultrapack TSK G-2000 SWG; 21.5 mm × 600 mm) with an exclusion limit of 200 000 Da. The proteins were eluted with 0.05 M acetate buffer, pH 4.0, at a flow rate of 3 mL/min. The HPLC purified material was dialyzed and lyophilized. The activity of HSPI was checked by radioimmunoassay.[6] The protein was then dissolved in sodium acetate buffer (pH = 4.5; 100 mM), and then the pH was adjusted to 3.0 by addition of HCl.

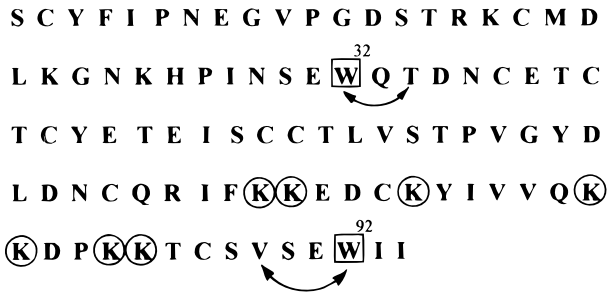

Figure 1. Amino acid sequence of the HSPI.[5] The two tryptophans at positions 32 and 92 are marked with squares, and the lysines nearer to W92 are marked with circles. The curved arrows represent the amino acids between which several nOe cross-peaks have been observed in the 2D NOESY NMR spectrum recorded in a mixed solvent of 90% H_2O and 10% ^2H_2O.

Other chemicals used in this study were acrylamide (Sisco Research Laboratories Co., India), KI (potassium iodide, Qualigens Fine Chemicals Co., India), CsCl (cesium chloride, Spectrochem Pvt. Ltd., India), sodium thiosulfate ($Na_2S_2O_3$, Qualigens Fine Chemicals Co., India), sodium acetate (Qualigens Fine Chemicals Co.), tryptophan (Sigma Chemical Co., United States), and NATA (*N*-acetyl tryptophanamide, Sigma

* Author for correspondence. Fax: 091-22-215 2110/2181. Tel: 091-22-215 2971/2979 (x 2489). Email: chary@tifrvax.tifr.res.in.

S1089-5647(97)03398-1 CCC: $15.00
Published on Web 06/18/1998

Chemical Co.). Doubly deionized water was used in the experiments. All the experiments on HSPI were carried out at pH 3.0.

Fluorescence Measurements. The steady-state fluorescence intensity and anisotropy measurements were carried out using SPEX Fluorolog 1681 T format spectrofluorophotometer. The time-resolved fluorescence measurements were made using a frequency-doubled output of a high repetition rate (800 kHz) picosecond dye laser (rhodamine 6G) coupled with a time-correlated single photon counting (TCSPC) setup described elsewhere,[7,8] currently using a microchannel plate photomultiplier (Hamamatsu 2809). The second harmonic output of the dye laser from an angle-tuned KDP crystal was used to excite the samples. The excitation wavelength was 295 nm to excite Trp preferentially. The emission was collected through a 320 nm cutoff filter to prevent detection of scattering of the excitation beam from the protein samples. The sample was excited with vertically polarized light and the fluorescence decay was collected with emission polarizer kept at the magic angle (≈54.7°) with respect to the excitation polarizer. For the anisotropy measurements, the fluorescence intensities were measured with the emission polarizer set at parallel or perpendicular orientation with respect to the excitation polarizer. Geometry factor (G-factor) for the TCSPC setup was determined by using the NATA in water whose rotational correlation time (0.09 ns) is faster than its fluorescence lifetime (2.98 ns). The instrument response function (IRF) was recorded using a magnesium oxide scattering solution. The full width at half-maximum (fwhm) of IRF is about 200 ps. Typical peak count in the emission decay for fluorescence intensity and anisotropy measurements was about 10 000, and the time per channel was 75.68 ps. All the experiments were carried out at 25 °C.

The experimentally measured fluorescence decay data is a convolution of the instrument response function with the intensity decay function. The intensity decay data was fitted to the appropriate equations by iterative reconvolution procedure using Levenberg−Marquardt algorithm for optimization of the parameters.[7,9,10] The fluorescence decay data collected at the magic angle were analyzed by *m*aximum *e*ntropy *m*ethod (MEM) as well as discrete exponential analysis.

In MEM, the decays were analyzed for the model of distribution of lifetimes.[11,12] In this, the intensity decay function is

$$I(t) = \int_0^{\tau_{max}} \alpha(\tau) \exp(-t/\tau)\, d\tau \qquad (1)$$

where $\alpha(\tau)$ is the distribution function that must be determined. In the analysis, above integral is approximated as a multi-exponential function of about 150 discrete lifetime values τ_i uniformly spaced in $\log(\tau)$ space (in our case, 10 ps to 10 ns), where the amplitudes α_i represent a continuous, smooth function. The optimum distribution is the one that fits the data with a χ^2 close to 1.0 and maximizes the Shannon−Jaynes entropy.[12]

In discrete exponential analysis, the intensity decay function was fitted to either a single- or a double-exponential function as

$$I(t) = \sum_i \alpha_i \exp\left(-\frac{t}{\tau_i}\right); \quad i = 1, 2 \qquad (2)$$

where α_i and τ_i are the amplitudes and the lifetimes. The polarized fluorescence decays (parallel and perpendicular) were fitted simultaneously[13] to obtain single set of parameters common to both the decays as

$$I_{\parallel} = {}^1/_3 I(t)[1 + 2r(t)]$$

$$I_{\perp} = {}^1/_3 I(t)[1 - r(t)] \qquad (3)$$

where *r(t)* is the anisotropy function which is single exponential in our case i.e.,

$$r(t) = r(0) \exp\left(-\frac{t}{\phi}\right) \qquad (4)$$

where $r(0)$ is the initial anisotropy and ϕ is the rotational correlation time. The goodness of the fits were judged by a χ^2 value close to 1 and the random residual distribution.

Fluorescence quenching studies were made using stock solutions (2.5 M) of the three quenchers acrylamide, KI, and CsCl prepared in acetate buffer. Small aliquots of the stock solutions were added to the protein solution (≈25 μM) to attain the desired concentration of the quencher, and the changes in the fluorescence intensity were measured. In the case of the quenching experiments with KI, the solution contained 100 μM sodium thiosulfate ($Na_2S_2O_3$) to avoid the formation of I_3^-. The changes in the steady-state intensity with the addition of the quencher were used to obtain the quenching rate constant using the Stern−Volmer equation[14,15]

$$I_0/I = 1 + K_{SV}[Q] \qquad (5)$$

where I_0 and I are the steady-state intensities in the absence of the quencher and at the quencher concentration [Q] and K_{SV} is the Stern−Volmer constant. The above equation is linear for purely dynamic or purely static quenching mechanisms. In the case of the pure dynamic quenching mechanism, the Stern−Volmer constant is equal to $k_q\tau_0$, where k_q is the dynamic quenching rate constant and τ_0 is the fluorescence lifetime in the absence of the quencher. K_{SV} becomes K_s, the association constant for the quencher with the fluorophore in the case of the static quenching mechanism. The equation can be used to calculate the quenching rate constant k_q or the association constant K_s depending on the quenching mechanism. The clear distinction between these two mechanisms can be made from the time-resolved measurements. The dynamic quenching mechanism is reflected in the changes in the lifetimes, whereas the static quenching mechanism does not change the lifetimes. The time-resolved quenching studies were carried out to elucidate the quenching mechanisms where the change in fluorescence lifetimes with the addition of the quenchers was used to obtain the dynamic quenching rate constants.

Decay Associated Spectra. In the case of biological systems such as proteins, where the fluorescence intensity decay is multiexponential, the method of DAS is commonly employed to obtain the spectra of individual lifetimes.[14] The procedure of global analysis of multiple files is done to obtain the common parameters to all the decays.[13]

For the purpose of global analysis, the fluorescence decays were collected at varying emission wavelengths 320 nm to 430 nm at 5 nm intervals with the sample excited at 295 nm. These decays were analyzed globally to obtain the lifetime parameters that are common to all the data sets and the amplitudes varying with the emission wavelength. The steady-state spectrum of the protein was resolved into the spectra of the individual lifetimes using the equation

$$I_i(\lambda) = I(\lambda)\frac{\alpha_i(\lambda)\tau_i}{\sum_i \alpha_i(\lambda)\tau_i} \qquad (6)$$

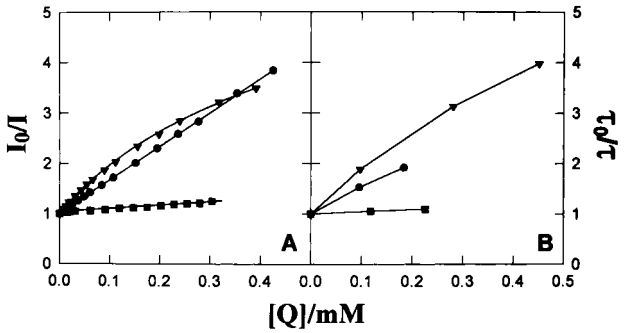

Figure 2. (A) Steady-state intensity Stern−Volmer plots. I_0 and I are the steady-state intensities without and with the addition of the quencher. (B) Lifetime Stern−Volmer plots. τ_0 and τ are the average lifetimes before and after the addition of the quencher. ● Acrylamide, ▼ KI, and ■ CsCl.

where I is the steady-state intensity and I_i and α_i are the steady-state intensity and the amplitude corresponding to the ith lifetime τ_i.

NMR Experiments. 2D NMR experiments were carried out on a Varian Unity$^+$ spectrometer with a ^{1}H frequency of 600 MHz. Though several 2D experiments have been recorded in ^2H_2O and in a mixed solvent of 90% H_2O + 10% ^2H_2O, we discuss only the *two q*uantum *f*iltered *co*rrelation spectroscop*y* (2QF COSY)[16] and *n*uclear *O*verhauser *e*nhancement spectroscop*y* (NOESY)[17] spectra in the present context. The experiments were carried out at pH 3.0 and temperature 20 °C with a protein concentration of 2.5 mM.

Results and Discussion

Fluorescence Quenching Studies. The Stern−Volmer (SV) plots derived from the steady-state measurements with three different quenchers, namely, acrylamide, KI, and CsCl, are shown in Figure 2A. It is evident that KI quenches the fluorescence most effectively. The efficiency of quenching is in the order KI > acrylamide ≫ CsCl. The Stern−Volmer quenching plots for acrylamide and CsCl are linear while the behavior for KI is nonlinear. The Stern−Volmer constants (K_{SV}) calculated in the case of acrylamide and CsCl are 6.68 and 0.79, M^{-1} respectively. The K_{SV} in the case of KI, calculated from the initial slope, is 11.42 M^{-1}.

Acrylamide is known to quench solvent-exposed as well as the buried tryptophans by penetrating through the rapidly fluctuating protein matrix.[18] The linear Stern−Volmer plot for acrylamide quenching in the case of HSPI indicates that the fluorescence is either from only one of the two Trp or both having identical local environment. Here, the use of different charged quenchers helps to identify the local environments of the two tryptophans in the protein. In the case of HSPI, KI quenches the fluorescence more efficiently compared to acrylamide and the SV plot shows a downward curvature. The downward curvature observed in the case of iodide quenching can be explained in terms of the two Trp having different quenching rate constants or the quenching mechanism involving both static and dynamic quenching.

Time-resolved fluorescence studies were carried out to obtain fluorescence lifetimes for the protein and to identify the fluorescence quenching mechanisms. The fluorescence intensity decay at 350 nm was collected at magic angle polarization, excited at 295 nm. The decay was analyzed by MEM to obtain the distribution of lifetimes. MEM does not assume any a priori model for the excited-state kinetics or lifetimes. It assumes initially that the lifetimes are distributed with equal probability (amplitude) in a range (typically, 10 ps to 10 ns in our case) and the shape of the distribution (amplitude vs lifetime) is obtained as the final outcome of the analysis.[12] If the fluorescence decay is truly a sum of exponentials, then MEM analysis gives a multimodal or multipeaked distribution. The resolvability of the multiple peaks depends on the signal-to-noise ratio of the fluorescence decay data.[19] Fluorescence intensity decay of HSPI in acetate buffer (pH 3.0) is shown in Figure 3. The inset in Figure 3 shows the result of MEM analysis of the fluorescence intensity decay of HSPI protein. The distribution clearly shows two well-resolved peaks. A comparison of the average lifetimes for the two peaks in the distribution of lifetimes with those obtained by discrete exponential analysis shows a one-to-one correspondence (Table 1 and Figure 3).

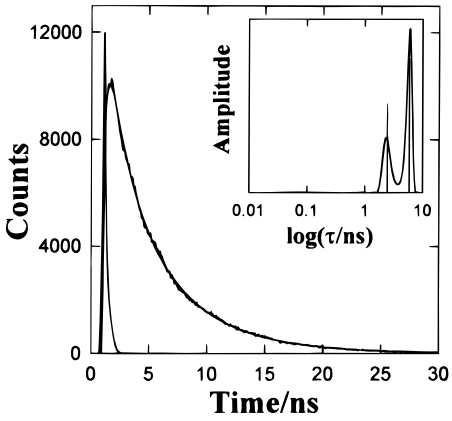

Figure 3. Fluorescence intensity decay of HSPI. The figure shows the excitation profile and the experimental and calculated intensity decays. The inset shows the results of this intensity decay data by discrete exponential analysis and MEM analysis. The vertical lines represent the two lifetimes obtained with the discrete analysis which are in one-to-one correspondence with the two peaks in the lifetime distribution obtained by MEM analysis.

TABLE 1: Analysis of Fluorescence Intensity Decay Data of HSPI in the Presence of Three Quenchers

quencher	[quencher]/mM	τ_1/ns	τ_2/ns	α_1	α_2	τ_m/ns
acrylamide	0	5.86	2.44	0.64	0.36	4.64
	95	3.91	1.61	0.62	0.38	3.04
	183	3.02	1.28	0.65	0.35	2.42
KI	97	3.11	1.30	0.64	0.36	2.46
	280	1.89	0.65	0.67	0.33	1.48
	450	1.40	0.44	0.76	0.24	1.17
CsCl	118	5.46	2.22	0.67	0.33	4.40
	225	5.13	2.05	0.71	0.29	4.24

The fluorescence decay of HSPI is biexponential with lifetimes of 5.86 and 2.44 ns, and the corresponding amplitudes are 0.64 and 0.36. Time-resolved fluorescence quenching studies were carried out to elucidate the quenching mechanisms. Table 1 shows the results of discrete exponential analysis on these fluorescence intensity decays in the presence of the three quenchers, which match well with those obtained by MEM analysis. The two lifetimes and the mean lifetime decrease by the addition of the three quenchers indicating that the quenching mechanism is dynamic in nature. The order of quenching efficiency is the same as determined by the steady-state intensity measurements: KI > acrylamide ≫ CsCl. The Stern−Volmer plots for the average lifetime variation are shown in Figure 2B. The SV plot for mean lifetime are linear for acrylamide and CsCl whereas it is nonlinear for KI, a result similar to the steady-state intensity plots. These results confirm that the quenching mechanism is purely dynamic.

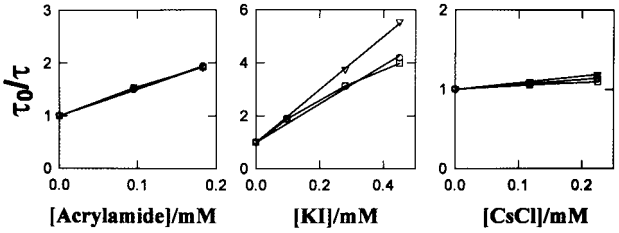

Figure 4. Dynamic Stern−Volmer plots for the three quenchers. ○ τ_{long} 5.86 ns, ▽ τ_{short} 2.44 ns, and □ τ_{av} 4.64 ns.

The Stern−Volmer plots for the individual lifetimes are shown in Figure 4. The plots are linear for both the lifetimes indicating that different tryptophans contribute to the two lifetimes. The quenching rate constants are calculated from the slopes of the Stern−Volmer plots and the lifetimes. The values for the long lifetime (5.86 ns) are 1.2×10^9 M^{-1} s^{-1} for KI, 0.9×10^9 M^{-1} s^{-1} for acrylamide, and 0.1×10^9 M^{-1} s^{-1} for CsCl; for the short lifetime (2.44 ns), they are 4.1×10^9 M^{-1} s^{-1} for KI, 2.1×10^9 M^{-1} s^{-1} for acrylamide, and 0.3×10^9 M^{-1} s^{-1} for CsCl. The value of the quenching rate constant for the short lifetime is consistently higher for all three quenchers: 2.3 (acrylamide), 3.4 (KI), and 3.0 (CsCl). These results are consistent with the model that the two lifetimes are associated with the two tryptophans in different local environments. Both are accessible to the solvent, and the one with a short lifetime is more solvent-accessible than the other.

Among the three quenchers, acrylamide is known to quench the Trp fluorescence more efficiently compared to KI and CsCl. The fluorescence quenching rate constants for these three fall in the order acrylamide > KI ≫ CsCl. The dynamic quenching rate constants for indole fluorescence for acrylamide, KI, and CsCl are 7.1×10^9, 6.4×10^9, and 1.1×10^9 M^{-1} s^{-1}, respectively.[20] In the case of HSPI, KI was the most efficient quencher. The increased quenching efficiency of KI can only be explained by attractive electrostatic interaction between the negatively charged quencher and the tryptophan region of the protein, which ought to be positively charged. The primary structure of HSPI (Figure 1) shows that there are seven lysine residues (marked in Figure 1 with circles) in the neighborhood of W92 and fewer positively charged residues near W32. The lysine residues whose side chain is positively charged (NH_3^+ group, pK_a 10.53 [21]) may constitute a positively charged pocket around W92, which increases the local concentration of negatively charged iodide compared to the bulk concentration.[22,20] This results in increased quenching efficiency for iodide compared to acrylamide. It was identified earlier that the quenching rate constant was higher for the short-lifetime component (2.44 ns). Therefore, one can associate the short lifetime of 2.44 ns with W92 and the long lifetime of 5.86 ns with W32. However, this assignment can be confirmed only by mutating the protein to eliminate one of the two tryptophans.

Decay-Associated Spectra of Tryptophans. The fluorescence emission maximum of tryptophan depends on the local environment in the protein, i.e., on the neighboring amino acid groups surrounding the tryptophan. The Trp emission maximum in water (completely exposed to solvent) occurs at 360 nm. If the Trp is in the hydrophobic region of the protein, the emission maximum gets blue-shifted to 310 nm.[14] The fluorescence emission maximum of HSPI occurs at 346 nm indicating that the Trp residues are significantly exposed to the solvent. As described earlier, the fluorescence of HSPI is due to two lifetimes that can be associated with different tryptophans. The steady-state fluorescence spectrum of HSPI was resolved into two spectra associated with the two lifetimes (DAS) as described

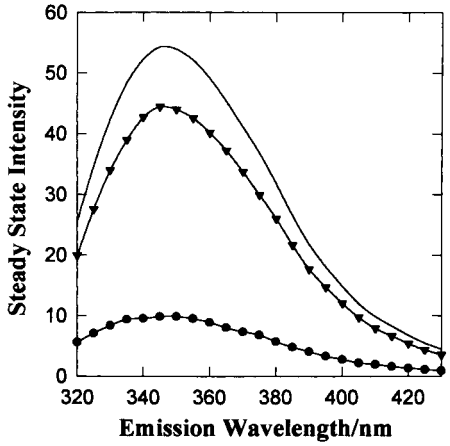

Figure 5. DAS of the two lifetimes of HSPI. The solid curve represents the steady-state intensity. The solid triangles and circles represent the spectra of the long (5.86 ns) and short lifetime (2.44 ns), respectively.

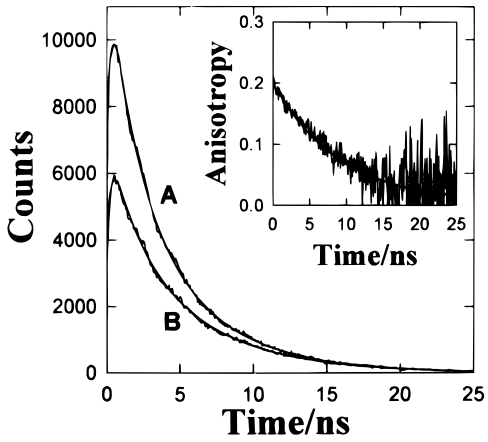

Figure 6. Polarized fluorescence intensity curves of HSPI. The figure shows the observed and fitted parallel and perpendicularly polarized intensity decays. The inset shows the time-resolved fluorescence anisotropy calculated from the above two decays.

in the "Materials and Methods" section. The fluorescence decays collected at emission wavelengths varying from 320 to 430 nm at an interval of 5 nm at the excitation wavelength 295 nm were analyzed globally to obtain the two lifetimes that are common to all the emission wavelengths and amplitudes as a function of the emission wavelength. The decay-associated spectra computed using eq 6 are shown in Figure 5. As seen in Figure 5, the emission maxima (345 nm) and the spectral shapes of both the lifetimes are identical. These results, together with the results of fluorescence quenching studies, confirm that the two tryptophans have a solvent-exposed environment.

Fluorescence Anisotropy and Dynamics of HSPI. The steady-state fluorescence anisotropy at $\lambda_{ex} = 295$ nm and $\lambda_{em} = 350$ nm is 0.117. Figure 6 shows the time-resolved fluorescence intensity decays collected with the emission polarizer kept parallel and perpendicular to the excitation polarizer. The inset in Figure 6 shows the anisotropy decay calculated from the above two polarized intensity decays. The time-resolved anisotropy decay can be fitted to a single-exponential function with rotational correlation time of 9.2 ns.

The fluorescence anisotropy in the case of proteins comes from two independent motions: rotational dynamics of the entire protein and segmental/local dynamics of the Trp residue(s). The anisotropy decay resulting from the rotational motion of the protein is single exponential if the protein is spherical. If it is nonspherical, the decay is multiexponential. The segmental/

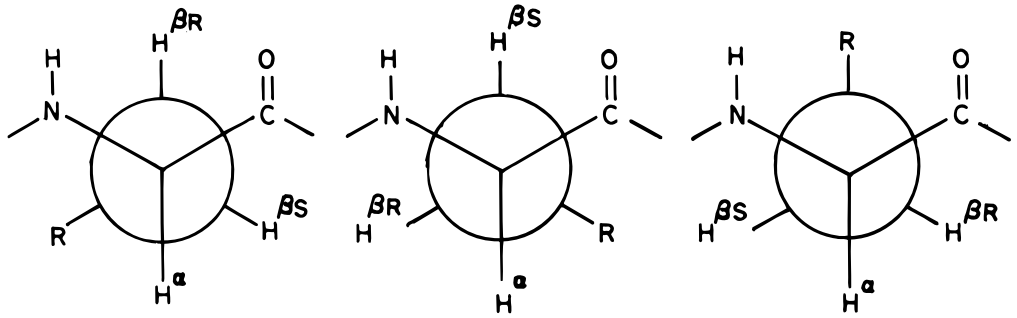

	$\chi^1=-60^0$	$\chi^1=+180^0$	$\chi^1=+60^0$
$J(H^{\alpha}\text{-}H^{\beta R})$	Large(~13.56 Hz)	Small(~2.6 Hz)	Small(~2.6 Hz)
$J(H^{\alpha}\text{-}H^{\beta S})$	Small(~2.6 Hz)	Large(~13.56 Hz)	Small(~2.6 Hz)
$COSY(H^{\alpha}\text{-}H^{\beta R})$	Strong	Weak	Weak
$COSY(H^{\alpha}\text{-}H^{\beta S})$	Weak	Strong	Weak
$nOe(H^{\alpha}\text{-}H^{\beta R})$	Weak	Strong	Strong
$nOe(H^{\alpha}\text{-}H^{\beta S})$	Strong	Weak	Strong

Figure 7. Three rotamer structures seen along $C_{\alpha}-C_{\beta}$ bond of tryptophan. The table indicates the expected $J(H^{a}-H^{bR}/H^{bS})$ values and COSY and NOESY cross-peak intensities between the H^{a} and H^{bR}/H^{bS} protons that one would observe for the above three rotamer structures.

local dynamics of the Trp residue consists of its side chain dynamics with or without a segment of the polypeptide. The local dynamics is generally described by the "wobbling-in-cone" model[23,24] where the Trp residue wobbles freely within a cone of semiangle related to the order of its environment. In view of the different types of depolarizing dynamics, it is more common to observe multiexponential anisotropy decay for proteins containing multiple tryptophans. The longest correlation time is ascribed to the rotational motion of the protein, and lower values to segmental and local dynamics of the tryptophan.

The time-resolved anisotropy of HSPI shows a single rotational correlation time of 9.2 ns, which is attributable to the rotational motion of the protein as a whole. The absence of fast correlation times in the anisotropy decay of this protein indicates the absence of segmental and local depolarizing dynamics. In other words, the indole moieties of both tryptophans are rigidly held in their respective spatial locations. This conclusion is confirmed by the NMR results as described in the next section.

The molecular mass of HSPI is 10.4 kDa. Assuming the shape of the protein to be spherical, the rotational correlation time ϕ can be calculated using Stokes−Einstein equation (eq 8) and hydrated molecular volume of the protein. The latter can be calculated using an empirical equation[25]

$$V_h = \frac{M}{6} \times 10^{-23}\ \text{cm}^3 \tag{7}$$

$$\phi = \frac{1}{6D_{rot}} = \frac{V_h \eta}{kT} \tag{8}$$

where ϕ is the rotational correlation time, D_{rot} is the rotational diffusion coefficient, V_h is the hydrated molecular volume of the protein, η is the viscosity of the medium, k is the Boltzmann constant, T is the absolute temperature, and M is the molecular weight of the protein. The calculated value of ϕ for HSPI is 4.4 ns, which is far less than the experimentally determined value of 9.2 ns. We consider three possibilities to account for the difference between the two values. (1) If the protein is aggregated in solution, then the rotational correlation time of the protein will be higher. In our case, a dimer of the protein will account for the experimental value of 9.2 ns. It is necessary though that the protein will have to be completely or very substantially dimerized at a protein concentration of 25 μM used for fluorescence experiments. However, NMR experiments carried out at a protien concentration of 2.5 mM (more favorable for dimerization) have not given any evidence for the existence of dimers. All the resonances, including NOESY and COSY cross-peaks, are accounted for by the primary sequence of the protein. SDS-PAGE gel electrophoresis of HSPI is also not in favor of the formation of dimer.[4] Hence, we rule out this attractive possibility. (2) The hydrated volume of the protein could be much larger than that calculated by the empirical eq 7. HSPI could be an exception to this generalization that hydrated specific volume is 1 cm^3/g of a typical protein.[25] If the protein is associated with one more additional layer of water molecules than that of typical proteins, the radius increases by 0.4 nm[26,27] and the volume of HSPI would increase by 95%. Then the calculated value of ϕ (8.6 ns) will be closer to the experimental value (9.2 ns). This possibilty is realistic because proteins with charged surfaces are known to be more hydrated than those with uncharged surfaces. (3) The third possibility is that the protein is nonspherical. If the protein is ellipsoidal (prolate or oblate), single-exponential anisotropy decay is still observed if the transition dipole is parallel to the symmetry axis.[28] The axial ratio for the prolate or oblate shape of HSPI that would give a rotational correlation time of 9.2 ns was computed to be 2.73 (prolate) and 0.21 (oblate). The circular dichroism spectrum of HSPI (not shown here), which indicates secondary structural elements such as β-sheets and β-turns, and preliminary NMR structure studies suggest that HSPI may be a prolate ellipsoid, like the case of α-amylase inhibitor.[29,30]

Rotamer Structures by NMR. As discussed earlier, the two fluorescence lifetimes, 5.86 and 2.44 ns, can be associated with the two tryptophans W32 and W92, respectively. There are only a few examples of multi-trp proteins for which it was possible to identify the lifetimes with individual tryptophans.[31,32] Multiexponential fluorescence decay is commonly observed in several proteins,[27] including many proteins containing only one tryptophan.[33,34,35,36] It is usually difficult to associate fluorescence lifetimes with individual tryptophans without modifying the protein to a simple single trp protein. Fluorescence anisotropy of HSPI has also revealed the compact structure of the protein devoid of segmental or local dynamics in the region of the tryptophan. This gives rise to the possibility that the indole moiety of tryptophan is held rigidly in one of three rotamer structures (see below), which can be unambiguously confirmed from NMR studies.

Tryptophan in water at pH 7 shows a biexponential fluorescence decay, and the lifetimes are assigned to rotamer structures.[27] Multiexponential decay of tryptophan fluorescence in proteins has been generally attributed to multiple conformations (χ^1 rotamers) around the $C^\alpha-C^\beta$ bond of the tryptophan side chain,[37,38] multiple microstates of the protein,[39] or multiple structures of the protein.[40,41] The recent work[42] on the lifetime distributions of single tryptophan proteins has strongly suggested that multiexponential decay of the tryptophan arises owing to the presence of various rotamers the tryptophan side chain can adopt. The two fluorescence lifetimes for the free tryptophan in water have been assigned to these rotamer structures about the $C^\alpha-C^\beta$ bond, which makes the indole group proximal to the carboxyl group in two of the three structures.[43] The three rotamer structures (χ^1 conformations whose structures are shown in Figure 7) are found to be long-lived on the millisecond time scale using NMR experiments.[44] Hence the three tryptophan rotamers would show up as distinctly different species in the nanosecond/picosecond time scale fluorescence lifetime experiments. The fluorescence decay of a tryptophan analogue that has restricted rotation about the $C^\alpha-C^\beta$ bond is found to be biexponential, which is correlated with the two conformational populations calculated from ^{1}H NMR coupling constants.[45,46] The combined study of fluorescence decay and NMR of tryptophan containing polypeptide has shown that the population of the three rotamers derived from NMR experiments were in excellent agreement with the amplitudes of the three fluorescence decay components.[44] All these strongly suggest that the fluorescence decay of a tryptophan in a protein depends on its relative populations of the three rotamers.

In light of the above discussion, the assignment of the two lifetimes to two individual tryptophans in HSPI implies that the two tryptophans are in sterically constrained environments and the tryptophan side chain is in a single conformation. The absence of fast decay in the fluorescence anisotropy is also in support of the argument that the tryptophans in HSPI are in rigid environments.

^{1}H NMR can be used to calculate the relative populations of the three rotamers (shown in Figure 7) from the experimental values of the coupling constants (J s) between H^α and $H^{\beta R}$ ($H^{\beta S}$), which in turn can be used to explain the fluorescence decay kinetics.[44] The estimation of these coupling constants is not straightforward except in the case of small peptides and proteins (containing less than 50 amino acids). For larger proteins, the 2D NMR spectral resolution suffers from extensive spectral overlaps, large resonance line widths, antiphase active coupling constants and inphase passive coupling constants. For HSPI with 94 amino acids, the conformational dependent characteristic multiplet structures of the individual COSY cross-peaks were not resolved and hence could not aid in the estimation of the J couplings. In situations where the J-couplings were less than the individual resonance line widths, corresponding COSY cross-peaks are either weak or absent. In view of this, we have made an attempt to qualitatively fix the χ^1 rotamer populations from the cross-peak patterns observed in the 2D NMR spectra of HSPI and compare them with the independent parameters obtained from the fluorescence experiments.

For a tryptophan side chain, the three most probable staggered rotamer conformations are with $\chi^1 = -60°$, $+180°$, and $+60°$ (Figure 7), and for all these rotamers, the $J(H^\alpha-H^{\beta R}, H^{\beta S})$ values are χ^1-dependent. They can be calculated for various values of χ^1 by using appropriate Karplus-type relations,[44] and these

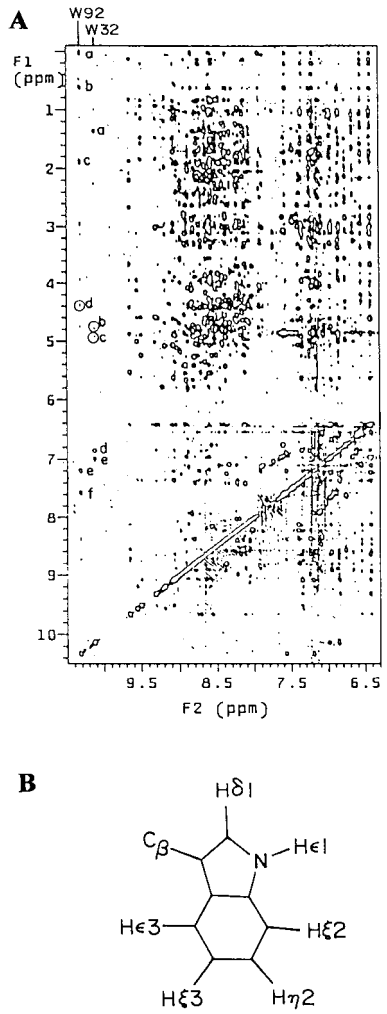

Figure 8. (A) Selected region of the water-gated NOESY spectrum of HSPI recorded in 90% H_2O + 10% ^2H_2O at 20 °C and pH 3.0. The nOe connectivities seen from various protons to the respective $N_{\epsilon 1}H$ protons of the two tryptophan side chains are highlighted with single character labels a−f. In the case of W32, the observed cross-peaks are from T34($C_\gamma H_3$) (a), T34($C_\beta H$) (b), T34($C_\alpha H$) (c), W32($C_{\delta 1}H$) (d), and W32($C_{\zeta 2}H$) (e) to W32($N_\epsilon H$), and in the case of W92, the cross-peaks observed are from V89($C_\gamma H_3$) (a), V89($C_\gamma H_3$) (b), V89($C_\beta H$) (c), V89($C_\alpha H$) (d), W92($C_{\delta 1}H$) (e), and W92($C_{\zeta 2}H$) (f) to W92($N_\epsilon H$). Experimental parameters: t_{1max} = 37.5 ms; t_{2max} = 256 ms; recycle delay = 1 s, 160 scans/t_1 increment, time-domain data points were 600 and 4096 along t_1 and t_2 dimensions, respectively. The data were multiplied with sine bell window functions shifted by $\pi/4$ and $\pi/8$ along t_1 and t_2 axes, respectively and zero-filled to 1024 data points along t1 dimension prior to 2D-FT. Digital resolution along ω_1 and ω_2 dimensions corresponds to 7.8 and 3.9 Hz/pt, respectively. (B) This shows the indole ring of tryptophan with the standard nomenclature used for identifying the hydrogen atoms.

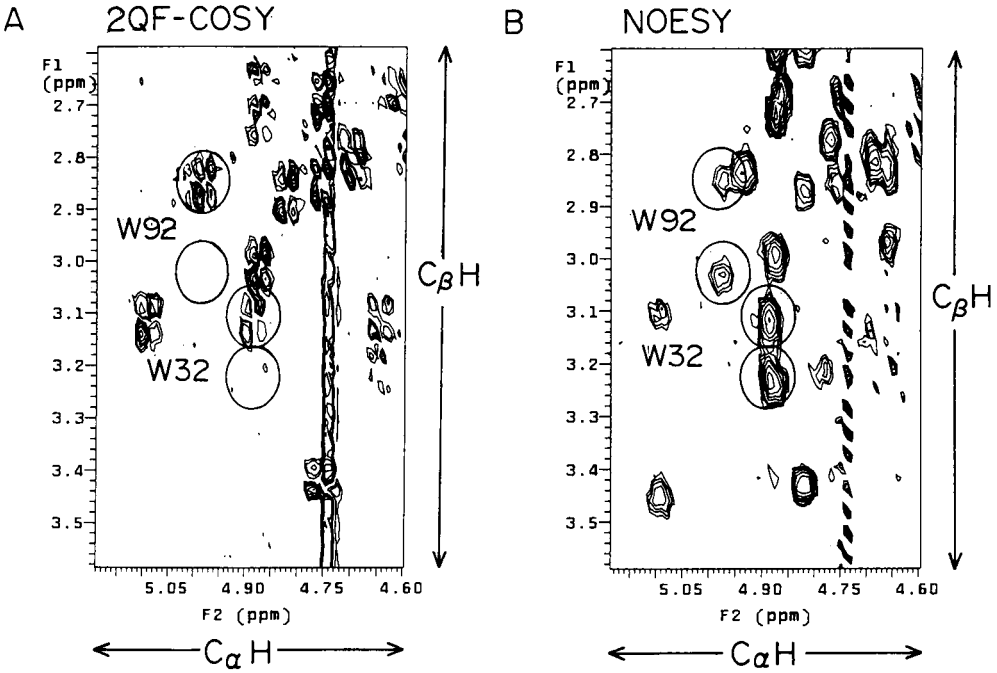

Figure 9. Selected spectral regions ($\omega_1 = 2.6-3.6$ ppm; $\omega_2 = 4.6-5.15$ ppm) of 600 MHz phase-sensitive 2QF COSY (A) and NOESY (B) spectra of HSPI (protein concentration 2.5 mM; pH 3.0; temperature 20 °C) showing through-bond (J) and through-space (nOe) connectivities, respectively, from $C_\beta H$ protons to $C_\alpha H$ protons. Experimental parameters for both these spectra were as follows: $t_{1max} = 46$ ms, $t_{2max} = 158$ ms, recycle decay = 1 s, 128 scans/t_1 increment, time-domain data points were 600 and 2048 along t_1 and t_2 dimensions, respectively. The mixing time (τ_m) in the case of NOESY was 150 ms. Both the data sets were multiplied with sine bell window functions shifted by $\pi/4$ and $\pi/8$ along t_1 and t_2 axes, respectively, and zero-filled to 1024 data points along the t_1 dimension prior to 2D-FT. Digital resolution along ω_1 and ω_2 dimensions corresponds to 6.44 and 3.22 Hz/pt, respectively. The *J* and nOe correlations arising from the $C_\alpha H$ and $C_\beta H$ protons of W32 and W92 are highlighted with circles around them. The absence of the *J* correlations in the COSY spectrum between the downfield shifted $C_\beta H$ protons and the $C_\alpha H$ protons of both the tryptophans is clearly evident. Though one of the nOe cross-peaks for W32 partially suffers from spectral overlaps, the nOe correlation from the downfield shifted $C_\beta H$ protons to $C_\alpha H$ protons are significantly stronger than the correlation from the upfield shifted $C_\beta H$ protons for both the tryptophans.

'J' values decide the COSY cross-peak intensities. Likewise, the nOe intensities between H^α and $H^{\beta R/\beta S}$ are also χ^1-dependent. Hence, the COSY and NOESY cross-peak intensities between H^α and $H^{\beta R}/H^{\beta S}$ protons can together be used to qualitatively fix the χ^1 populations and to know whether the tryptophan is in a single staggered rotamer conformation or not.

For a staggered rotamer conformation with $\chi^1 = -60°$ and $\chi^1 = +180°$, the COSY cross-peak between H^α and one of the H^β protons is very intense, while the cross-peak with the other β proton is at the same time below the lowest contour level because of the coupling constants involved (trans protons show a large coupling constant compared to the gauche protons) (see Figure 7). On the other hand, the COSY cross-peaks between the H^α and $H^{\beta R}/H^{\beta S}$ for the rotamer population with $\chi^1 = +60°$ will be of the same intensity. Similarly the NOESY cross-peak intensities between H^α and $H^{\beta R}/H^{\beta S}$ protons are also χ^1-dependent. For $\chi^1 = -60°$ and $+180°$, the H^β proton that is in trans orientation with respect to the H^α proton expectedly shows weaker nOe compared to the other H^β proton that is in the gauche ($g^\pm$) conformation with respect to the H^α proton. For the other conformation ($\chi^1 = +60°$), both the NOESY cross-peaks between the H^α and H^β protons are equal and strong in intensity. In the event of rotational averaging between the three rotamer conformations about the $C^\alpha-C^\beta$ bond, the $J(H^\alpha, H^{\beta R})$ and $J(H^\alpha, H^{\beta S})$ values average out and result in equal cross-peak intensities between H^α and $H^{\beta R}/H^{\beta S}$. Similarly, interproton distances between H^α and $H^{\beta R}/H^{\beta S}$ also average out and result in equal nOe cross-peak intensities between H^α and $H^{\beta R}/H^{\beta S}$ in the NOESY spectrum. It is very difficult to differentiate this rotational averaging with the case where the single rotamer with $\chi^1 = +60°$ is populated because, in both the cases, the COSY and NOESY cross-peak intensities between H^α and $H^{\beta R}/H^{\beta S}$ protons are similar.

One-dimensional spectrum and various two-dimensional spectra of HSPI recorded in ^2H_2O and in a mixed solvent of 90% H_2O + 10% ^2H_2O were used to assign the individual amino acids and their connectivities.[5] Briefly, the spin systems of the amino acid residues in HSPI were identified using 2D NMR spectra recorded in ^2H_2O solution, which was followed by sequence-specific resonance assignments using standard strategies.[47] The procedures involve identifying individual amino acid spin systems using 2D J-correlated spectroscopy (COSY) followed by detection of sequential cross-peaks arising from short interproton distances (d_{NN}, $d_{\alpha N}$, $d_{\beta N}$, etc.) between the immediate (sequential) neighbors in the NOESY spectrum. The $N_\epsilon H$ protons of the two tryptophans (W32 and W92) present in HSPI are easily identifiable because of their inherent chemical shift, which is most downfield shifted (10.3 ppm) in the ^1H spectrum. Figure 8 shows the nOe connectivities to the side chain $N_\epsilon H$ of the two tryptophans from their respective $C_{\delta 1}H$ and $C_{\zeta 2}H$ protons. These were the starting points in this resonance assignment procedure. The distinction between the $C_{\delta 1}H$ and $C_{\zeta 2}H$ protons has been achieved from the observation of $N_\epsilon H-C_{\delta 1}$ H cross-peak in the TOCSY spectrum recorded in a mixed solvent of 90% H_2O + 10% ^2H_2O (not shown here). $N_\epsilon H$ and $C_{\zeta 2}H$ are not *J*-coupled and hence do not show mutual interaction in the TOCSY spectrum. However, since the interproton distance between $N_\epsilon H$ and $C_{\zeta 2}H$ is 2.84 Å, one observes strong nOe between these protons, which helps in the identification of the $C_{\zeta 2}H$ proton (Figure 8). From the knowledge of $C_{\zeta 2}H$ position, the rest of the indole ring protons have been assigned from the combined use of NOESY and

TOCSY spectra in ^2H_2O. Further, the intraresidue nOes $C_{\delta 1}H$ to $C_\alpha H$ and $C_\beta H$ protons and $C_\alpha H$ to NH (backbone) allowed complete identification of the remaining protons of both the tryptophans.[5] With this knowledge, nOe cross-peaks corresponding to sequential distances (d_{NN}, $d_{\alpha N}$, $d_{\beta N}$, etc.) between neighboring amino acid residues were assigned. This led to assignment of glutamine (Q33) and isoleucine (I93) spin systems,[5] as sequential neighbors of W32 and W92, respectively. Sequential connectivities of Q33 and I93 with T34 and I94, respectively, further confirm these assignments.[5] The assignment described above (details in ref 5) led to the observation of only one set of resonances for each amino acid present in the protein. For example, we see resonances coming from only two tryptophans, four tyrosines, two phenylalanines, and so forth. This observation strongly support that the protein exists in monomeric form at this concentration (2.5 mM).

Figure 9 shows the cross-peak patterns observed in the 2QF COSY (A) and NOESY (B) spectra of HSPI between the H^α and H^β protons of the two tryptophans. For both W32 and W92, the 2QF COSY spectrum (Figure 9A) shows only one cross-peak between one of the $C_\beta H$ protons and $C_\alpha H$ proton. The upfield shifted $C_\beta H$ protons show up strong *J* correlation to the $C_\alpha H$ proton while the downfield shifted ones do not. Such an observation directly indicates that the side chains of these residues are locked in a single staggered rotamer conformation, which is either with $\chi^1 = -60°$ or $+180°$. The NOESY spectrum of HSPI (Figure 9B) also shows different nOe intensities between the H^α and H^β protons for the two tryptophans. The downfield shifted $C_\beta H$ protons show a strong nOe with the C_α protons compared to the upfield shifted $C_\beta H$ protons. The trend in the intensities of the COSY and NOESY cross-peaks for the two tryptophans is as explained in the previous paragraphs. That is, the β proton which shows a strong COSY cross-peak (which is in trans conformation) with the α proton shows a weak NOESY cross-peak and vice versa. This substantiates our earlier conclusion that the tryptophan side chains are locked in a single staggered rotamer conformation. To further differentiate between the two possible rotamer conformations with $\chi^1 = -60°$ and $+180°$, one would require stereospecific resonance assignments of all the $C_\beta H$ protons of both the tryptophans.

The 2D NOESY NMR spectrum of HSPI recorded in a mixed solvent of 90% H_2O and 10% ^2H_2O (Figure 8) gives further evidence to show that each of the two tryptophans exists in single rotamer populations in their local environment. The spectrum shows a strong nOe cross-peak between ϵNH of W32 and $C_\gamma H_3$ of T34 and weak nOe cross-peaks between ϵNH of W32 and $C_\alpha H$ and $C_\beta H$ of T34, indicating that the tryptophan W32 is in close proximity to the threonine T34. Likewise, the other tryptophan W92 is found to be in close proximity to V89, from the observation of nOes from W92(ϵNH) to V89($C_\beta H$, $C_\gamma H_3$) (Figure 8). Further, as there are no other nOes seen arising from both the NϵH protons of W32 and W92, it clearly demonstrates that the two tryptophans in HSPI exist in single rotamer conformations in their respective sites.

Conclusions

The fluorescence decay of HSPI is biexponential and the two lifetimes are associated with two individual tryptophans (W92 and W32) based on steady-state and time-resolved fluorescence quenching studies. The decay-associated spectra and accessibility of tryptophans to fluorescence quenchers confirmed that the tryptophans are solvent-exposed. Increased quenching efficiency of potassium iodide indicated that both the tryptophans are in the region of positively charged surface of the protein. Fluorescence anisotropy results indicated that HSPI is a protein of compact structure, devoid of segmental/local motion for the tryptophan residues. NMR results confirm that the two tryptophan residues are present as single rotamer populations.

Acknowledgment. We thank the Late Dr. A. R. Sheth, Dr. S. B. Moodbidri, and Mr. M. S. Kadam for their help provided during the course of isolation and purification of HSPI. The facilities provided by the National Facility for High Field NMR, Tata Institute of Fundamental Research, Mumbai are gratefully acknowledged.

References and Notes

(1) Thakur, A. N.; Vaze, A. Y.; Dattatreyamurthy, B.; Sheth, A. R. *Ind. J. Exp. Biol.* **1981**, *19*, 307.
(2) Garde, S.; Sheth, A. R.; Lohiya, N. K.; Shah, M. G. *J. Biosci.* **1992**, *17*, 67.
(3) Moodbidri, S. B.; Hurkadli, K. S.; Sheth, A. R. *Ind. J. Exp. Biol.* **1989**, *27*, 214.
(4) Seidah, N. G.; Arbatti, N. J.; Rochemont, J.; Sheth, A. R.; Chretian, M. *FEBS Lett.* **1984**, *175*, 349.
(5) Rastogi, V. K.; Chary, K. V. R.; Govil, G. *Curr. Sci.* **1997**, *72*, 69.
(6) Liang, Z. G.; Kamada, M.; Koide, S. S. *Biochem. Biophys. Res. Commun.* **1991**, *180*, 356.
(7) Periasamy, N.; Doraiswamy, S.; Maiya, G. B.; Venkataraman, B. *J. Chem. Phys.* **1988**, *88*, 1638.
(8) Bankar, K. V.; Bhagat, V. R.; Das, R.; Doraiswamy, S.; Ghangrekar, A. S.; Kamat, D. S.; Periasamy, N.; Srivatsavoy, V. J. P.; Venkatarman, B. *Indian J. Pure Appl. Chem.* **1989**, *27*, 416.
(9) Grinvald, A.; Steinberg, I. Z. *Anal. Biochem.* **1974**, *59*, 583.
(10) Bevington, P. R.; Robinson, D. K. *Data Reduction and Error Analysis for the Physical Sciences*, 2nd ed.; McGraw-Hill Inc.: New York, 1994.
(11) Livesey, A. K.; Brochon, J. C. *Biophys. J.* **1987**, *52*, 693.
(12) Brochon, J. C. *Methods Enzymol.* **1994**, *240*, 262.
(13) Knutson, J. R.; Beechem, J. M.; Brand, L. *Chem. Phys. Lett.* **1983**, *102*, 501.
(14) Lakowicz, J. R. *Principles of Fluorescence Spectroscopy*; Plenum Press: New York, 1983.
(15) Eftink, M. R. Fluorescence quenching: Theory and applications. In *Topics in Fluorescence Spectroscopy*; Lakowicz, J. R., Ed.; Plenum Press: New York 1991; pp 53−126.
(16) Rance, M.; Sorensen, O. W.; Bodenhausen, G.; Wagner, G.; Ernst, R. R.; Wuthrich, K. *Biochem. Biophys. Res. Commun.* **1983**, *117*, 479.
(17) Kumar, A.; Wagner, G.; Ernst, R. R.; Wuthrich, K. *Biochem. Biophys. Res. Commun.* **1980**, *96*, 1156.
(18) Eftink, M. R.; Ghiron, C. A. *Biochemistry* **1976**, *15*, 672.
(19) Swaminathan, R.; Periasamy, N. *Proc. Indian Acad. Sci.: Chem. Sci.* **1996**, *108*, 39.
(20) Eftink, M. R.; Ghiron, C. A. *Anal. Biochem.* **1981**, *114*, 199.
(21) Lehninger, A. L.; Nelson, D. L.; Cox, M. M. In *Principles of Biochemistry*; CBS Publishers and Distributors: India, 1993; Chapter 5, p 113.
(22) Lehrer, S. S. *Biophys. J.* **1971**, *11*, 72a.
(23) Kinosita, K. J.; Kawato, S.; Ikegami, A. *Biophys. J.* **1977**, *20*, 289.
(24) Lipari, G.; Szabo, A. *Biophys. J.* **1980**, *30*, 489.
(25) Cantor, C. R.; Schimmel, P. R. In *Biophysical Chemistry*; W. H. Freeman and Co.: New York, 1980; Chapter 8, p 461.
(26) Brochon, J. C.; Wahl, P.; Auchet, J. C. *Eur. J. Biochem.* **1974**, *41*, 577.
(27) Beechem, J. M.; Brand, L. *Annu. Rev. Biochem.* **1985**, *54*, 43.
(28) Fleming, G. R. In *Chemical Applications of Ultrafast Spectroscopy*; Oxford University Press: New York, 1986; Chapter 6, p 130.
(29) Pflugrath, J.; Wiegand, E.; Huber, R.; Vertesy, L. *J. Mol. Biol.* **1986**, *189*, 383.
(30) Kline, A. D.; Braun, W.; Wuthrich, K. *J. Mol. Biol.* **1988**, *204*, 675.
(31) Ross, J. B. A.; Schmidt, C. J.; Brand, L. *Biochemistry* **1981**, *20*, 4369.
(32) Borkman, R. F.; Douhal, A.; Yoshihara, K. *Biochemistry* **1993**, *32*, 4787.
(33) Waldman, A. D. B.; Clarke, A. R.; Wigley, D. B.; Hart, K. W.; Chia, W. N.; Barstow, D.; Atkinson, T.; Munro, I.; Holbrook, J. J. *Biochim. Biophys. Acta* **1987**, *913*, 66.
(34) Shen, W. H. *Biochemistry* **1993**, *32*, 13925.
(35) Willaert, K.; Loewenthal, R.; Sancho, J.; Froeyen, M.; Fersht, A.; Engelborghs, Y. *Biochemistry* **1992**, *31*, 711.

(36) Swaminathan, R.; Nath, U.; Udgaonkar, J. B.; Periasamy, N.; Krishnamoorthy, G. *Biochemistry* **1996**, *35*, 9150.
(37) Chen, L. X. Q.; Longworth, J. W.; Fleming, G. R. *Biophys. J.* **1987**, *51*, 865.
(38) Chen, R. F.; Knutson, J. R.; Ziffer, H.; Porter, D. *Biochemistry* **1991**, *30*, 5184.
(39) Harris, D. L.; Hudson, B. S. *Biochemistry* **1990**, *29*, 5276.
(40) Chabbert, M.; Hillen, W.; Hansen, D.; Takahashi, M.; Bousquet, J. A. *Biochemistry* **1992**, *31*, 1951.
(41) Kim, S. J.; Chowdhury, F. N.; Younathan, W. S. E. S.; Rosso, P. S.; Barkley, M. D. *Biophys. J.* **1993**, *65*, 215.
(42) Swaminathan, R.; Krishnamoorthy, G.; Periasamy, N. *Biophys. J.* **1994**, *67*, 2013.
(43) Szabo, A. G.; Rayner, D. M. *J. Am. Chem. Soc.* **1980**, *102*, 554.
(44) Ross, J. B. A.; Wyssbrod, H. R.; Porter, R. A.; Schwartz, G. P.; Michaels, C. A.; Laws, W. R. *Biochemistry* **1992**, *31*, 1585.
(45) Colucci, W. J.; Tilstra, L.; Sattler, M. C.; Fronczek, F. R.; Barkley, M. D. *J. Am. Chem. Soc.* **1990**, *112*, 9182.
(46) McMahon, L. P.; Colucci, W. J.; McLaughlin, M. L.; Barkley, M. D. *J. Am. Chem. Soc.* **1992**, *114*, 8442.
(47) Wuthrich, K. *NMR of Proteins and Nucleic Acids*; Wiley: New York, 1986.